

# Galaxy And Mass Assembly (GAMA): The effect of galaxy group environment on active galactic nuclei

Y. A. Gilletti<sup>1\*</sup>, K. A. Pihlström<sup>1</sup>, M. S. Owers<sup>1</sup>, J. S. B. Hlavica<sup>2,3</sup>, S. B. Gallagher<sup>4</sup>, M. J. I. Bower<sup>5</sup>, M. E. Chisholm<sup>6</sup>, S. M. Croom<sup>7</sup>, B. W. Hlavica<sup>8,9</sup>, J. L. Greig<sup>10</sup>, S. M. Jarvis<sup>10</sup>, D. Lyth<sup>11</sup>

- <sup>1</sup>E. A. Milne Centre for Astrophysics, University of Hull, Cottingham Road, Kingston-upon-Hull HU6 7RX, U.K.
- <sup>2</sup>Department of Physics and Astronomy, Macquarie University, NSW 2109, Australia
- <sup>3</sup>Australian Astronomical Observatory, 105 Dehli Road, North Ryde, NSW 2113, Australia
- <sup>4</sup>Sydney Institute for Astronomy (SIfA), School of Physics, The University of Sydney, NSW2006, Australia
- <sup>5</sup>School of Physics, University of New South Wales, NSW2052, Australia
- <sup>6</sup>School of Physics and Astronomy, Monash University, Clayton, Victoria 3800, Australia
- <sup>7</sup>Department of Physics and Astronomy, University of the Western Cape, Robert Sobukwe Road, Bellville, 7535, South Africa
- <sup>8</sup>Department of Physics and Astronomy, University of Louisville, Louisville KY 40292, U.S.A.
- <sup>9</sup>University of Leiden, Sterrenwacht Leiden, Niels Bohrweg 2, NL-2333 CA Leiden, The Netherlands
- <sup>10</sup>Astronomy Centre, University of Sussex, Falmer, Brighton BN1 9QH, U.K.
- <sup>11</sup>Indian Institute of Science Education and Research Mohali (IISERM), Knowledge City, Sector 81, SAS Nagar, Manauli PO 140306, India
- <sup>12</sup>SRON Netherlands Institute for Space Research, Landleven 12, 9747 AD, Groningen, The Netherlands
- <sup>13</sup>Kapteyn Astronomical Institute, University of Groningen, Postbus 800, 9700 AV, Groningen, The Netherlands

2018 Jan 0. Received 2017 Dec 10; in final form 2018 Jan 0

## ABSTRACT

We investigate the effect of galaxy group environment on the occurrence of active galactic nuclei (AGN) in the Galaxy And Mass Assembly (GAMA) survey. We identify 451 AGN in the GAMA sample with  $z < 0.15$ . By comparing the AGN frequency in galaxy groups with  $r < 19.8$  arcmin to the AGN frequency in the field, we find that the AGN frequency in galaxy groups is  $3.6\sigma$  above the field level for  $10(M_{200}/M_{\odot}) > 9.9$  and  $0.53 \leq 10(M_{200}/M_{\odot}) \leq 14.56$ . This result is consistent with the theoretical prediction that AGN frequency increases with galaxy group mass. We find that the AGN frequency in galaxy groups is  $3.6\sigma$  above the field level for  $10(M_{200}/M_{\odot}) > 13.5$ , which is consistent with the theoretical prediction that AGN frequency increases with galaxy group mass.

Key words: Galaxy groups – Galaxy clusters – Active galactic nuclei

## 1 INTRODUCTION

Active galactic nuclei (AGN) are thought to be powered by accretion onto a supermassive black hole (SMBH) in the central galaxy of a galaxy group or cluster. The AGN frequency is expected to increase with galaxy group mass (Madau & Fick 1996; Madau & Fick 1996).

AGN frequency is expected to increase with galaxy group mass (Madau & Fick 1996; Madau & Fick 1996). The AGN frequency is expected to increase with galaxy group mass (Madau & Fick 1996; Madau & Fick 1996).

\* E-mail: y.gilletti@hull.ac.uk (YAG)

© 0000 RAS



2011). We use the GAMA  $z < 0.6$  TDS (75029 galaxies) with  $N_{FF} = 14876$  (Abel 882, Osh 2013).

We define the GAMA  $z < 0.15$  TDS (723 galaxies) with  $N_{FF} = 10$ .

### 2.2.2 Group membership

We use the  $G^3Cv09$  (Ritch 2011). Here we use the  $R_{200}$  (Cai 1997),

$$R_{200} = \frac{\sqrt{3}\sigma_p}{10H(z)}, \quad (1)$$

$$M_{200} = \frac{\sigma_p^3}{1090^3 h(z)} 10^{15} M_\odot \quad (2)$$

We use the  $N_{FF} \geq 5$  (Ritch 2011) galaxies with  $R_{200} \leq 0.5R_{200}$  (Cai 1997).

At the group level, we use the  $N_{FF} \geq 5$  (Ritch 2011) galaxies with  $R_{200} \leq 0.5R_{200}$  (Cai 1997).

$$V_i = (R/R_{200}) < \sqrt{\frac{2}{R/R_{200}} \frac{h_1 + \kappa R/R_{200} - (\kappa R/R_{200})/(1 + \kappa R/R_{200})}{h_1 + \kappa - \kappa/(1 + \kappa)}} \quad (3)$$

$$\kappa(M_{200}, z) = \frac{9.59}{1 + z_p} \left( \frac{M_{200}}{10^{14} M_\odot h^{-1}} \right)^{-0.102} \quad (4)$$

$$z_p = \frac{1}{10} \quad V_{200} = \sqrt{GM_{200}/R_{200}}$$

$^3Cv09$ ,

$$C = \frac{(cz_k - cz_p)^2}{\sigma_p^2} - 4 \log_{10} \left( 1 - \frac{R}{R_p} \right) \quad (5)$$

We use the  $R_p \leq 0.5R_{200}$  (Cai 1997) galaxies with  $N_{FF} \geq 5$  (Ritch 2011).

### 2.2.3 Group substructure

We use the  $\Delta$  (D&S 1988) to measure the group substructure.

The  $\Delta$  is defined as  $\Delta = \sum \delta_i$ , where  $\delta_i = \frac{n+1}{\sigma_b} [(v_b - v_i)^2 + (\sigma_b - \sigma_i)^2]$ .

$$\delta_i^2 = \frac{n+1}{\sigma_b} [(v_b - v_i)^2 + (\sigma_b - \sigma_i)^2] \quad (6)$$

We use the  $\Delta$  to measure the group substructure. The  $\Delta$  is defined as  $\Delta = \sum \delta_i$ .

$$n = \sqrt{N_{R < R_{200}}} \cdot A \cdot p$$

$$p = N(\Delta_{MC} > \Delta_b) / N(MC)$$

We use the  $\Delta$  to measure the group substructure. The  $\Delta$  is defined as  $\Delta = \sum \delta_i$ .

We use the  $\Delta$  to measure the group substructure. The  $\Delta$  is defined as  $\Delta = \sum \delta_i$ .

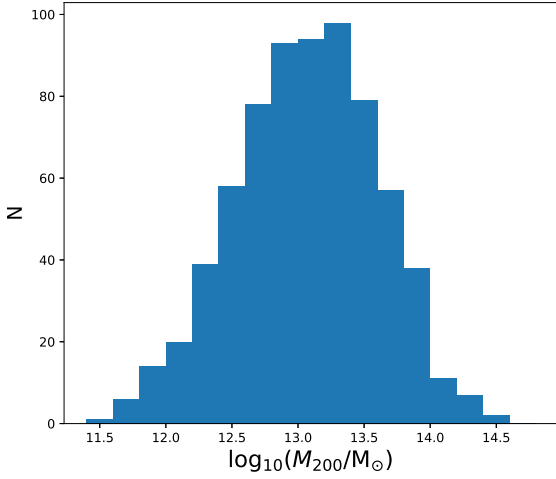
## 2.3 AGN selection

### 2.3.1 A complete AGN sample

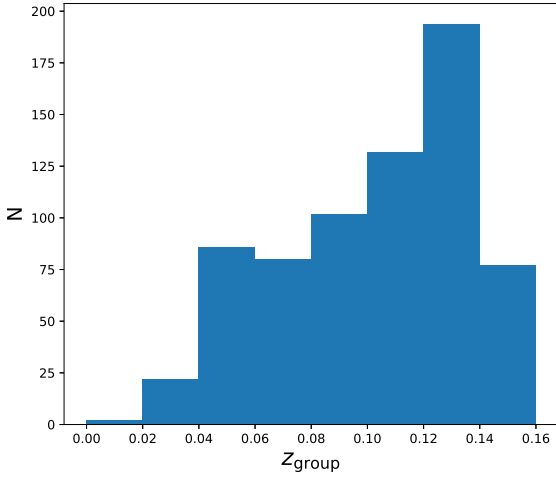
We use the GAMA AGN sample (Graham 2017) with  $N_{FF} \geq 5$  (Ritch 2011).

**Table 1.** The mean and standard deviation of the physical properties of the AGN sample.

Property	Mean	Standard Deviation	Min	Q <sub>1</sub>	Q <sub>2</sub>	Q <sub>3</sub>	Max
$N$	21.49	26.89	5.00	9.00	15.00	25.00	418.00
$\sigma_p$ [kpc]	248	103	69	173	228	304	718
$R_{200}$ [kpc]	548	226	159	381	504	675	1567
$\log_{10}(M_{200}/M_{\odot})$	13.06	0.54	11.53	12.71	13.07	13.45	14.56



(a)



(b)

**Figure 1.** The distribution of  $M_{200}$  (a) and  $Z_{\text{group}}$  (b) for the AGN sample.

$$\log_{10} \left( \frac{[\text{O III}] \lambda 5007}{\text{H}\beta} \right) > \frac{0.61}{\log_{10} \left( \frac{[\text{N II}] \lambda 6583}{\text{H}\alpha} \right) - 0.47} + 1.19 \quad (7)$$

The AGN sample is defined by the following criteria (Baldwin 1981):

$$\log_{10} \left( \frac{[\text{O III}] \lambda 5007}{\text{H}\beta} \right) > \beta, \quad [\text{O III}] \lambda 5007, \text{H}\alpha, [\text{N II}] \lambda 6583 / \text{H}\alpha >$$

### 3. AGN Selection

Following Cifuentes (2010),

we define

AGN as BPT objects

with  $S/N > 3$  in  $[\text{N II}] \lambda 5007$ , and

those with

Kew (2001) as AGN.

Using Cifuentes (2010) as

AGN objects

with  $\alpha$  of  $[\text{N II}] \lambda 6583$ . Using

AGN

with  $\alpha$ . This is the 'AGN'

of Cifuentes (2011) as

(ELG) as

- AGN,  $\log_{10} \left( \frac{[\text{N II}] \lambda 6583}{\text{H}\alpha} \right) < -0.4$
- AGN,  $\log_{10} \left( \frac{[\text{N II}] \lambda 6583}{\text{H}\alpha} \right) > -0.4$  and  $\text{H}\alpha < 6 \text{ \AA}$
- AGN,  $\log_{10} \left( \frac{[\text{N II}] \lambda 6583}{\text{H}\alpha} \right) > -0.4$  and  $\text{H}\alpha > 6 \text{ \AA}$

AGN', and

the AGN, the AGN as

defined by Cifuentes (2011).

AGN with  $\text{H}\alpha < 3 \text{ \AA}$  as

AGN, and WHAN as

AGN objects

with  $n_Q \geq 3$ , i.e. at least

3 of the following lines

(Dich 2011; Liu 2015). We

use  $\alpha$  of  $[\text{N II}] \lambda 6583$  in the

AGN

AGN

AGN

AGN

AGN (Gala 2017) as

AGN

AGN

AGN

The 2864 AGN

7498 AGN

AGN

AGN

AGN

AGN

AGN

AGN

AGN

AGN

AGN

AGN

AGN

AGN

AGN

AGN

AGN

$$S_{\text{H}\alpha, \text{AGN}} = S_{\text{H}\alpha, \text{AGN}} \left( \frac{\text{EW}_{\text{H}\alpha} + 2.5 \text{ \AA}}{\text{EW}_{\text{H}\alpha}} \right) \quad (8)$$

<sup>1</sup> AGN as

AGN (Hew 2013); as

AGN (GAMA AGN

AGN (GAMA AGN

AGN (GAMA AGN

AGN (GAMA AGN

AGN (GAMA AGN

AGN (GAMA AGN

AGN (GAMA AGN

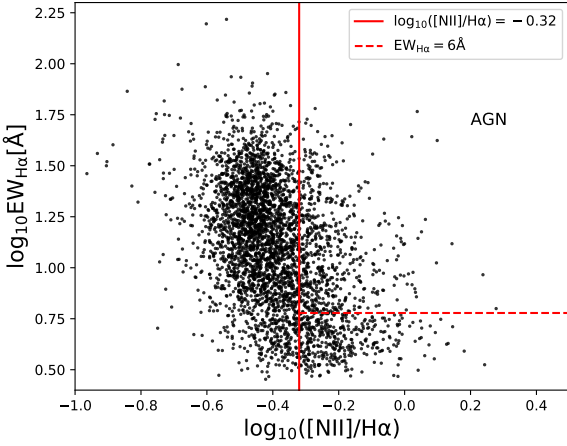


Figure 2. A WHAN selection criterion for AGN. The solid red line is  $\log_{10}([\text{N II}]/\text{H}\alpha) = -0.32$  and the dashed red line is  $\log_{10}(\text{EW}_{\text{H}\alpha}/\text{\AA}) < 0.5$ , and the region to the right of the solid line and above the dashed line is labeled AGN.

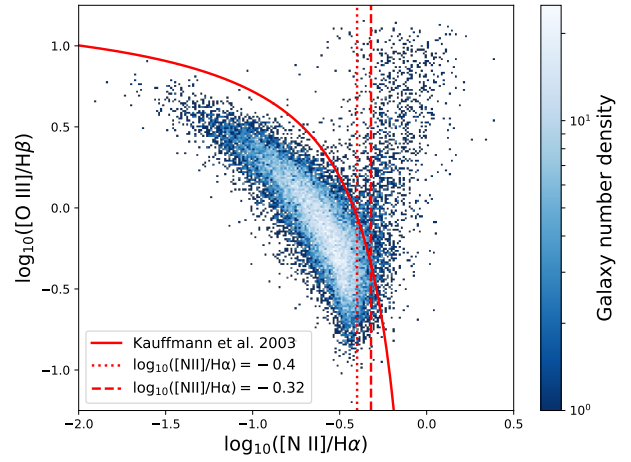


Figure 3. A BPT selection criterion for AGN. The solid red curve is the Kauffmann et al. (2003) AGN selection criterion. The vertical dashed red line is  $\log_{10}([\text{N II}]/\text{H}\alpha) = -0.4$  and the horizontal dashed red line is  $\log_{10}([\text{N II}]/\text{H}\alpha) = -0.32$  and the region to the right of the solid curve and above the dashed lines is labeled AGN.

2.3.1. Sample contamination

### 2.3.2 Sample contamination

AGN selection criteria are based on the [N II]  $\lambda 6583$  H $\alpha$  ratio and the [O III]  $\lambda 5007$  H $\beta$  ratio. The AGN selection criteria are based on the [N II]  $\lambda 6583$  H $\alpha$  ratio and the [O III]  $\lambda 5007$  H $\beta$  ratio. The AGN selection criteria are based on the [N II]  $\lambda 6583$  H $\alpha$  ratio and the [O III]  $\lambda 5007$  H $\beta$  ratio.

$$\log_{10}\left(\frac{[\text{O III}]\ \lambda 5007}{\text{H}\beta}\right) < \frac{0.61}{\log_{10}\left(\frac{[\text{N II}]\ \lambda 6583}{\text{H}\alpha}\right) - 0.05} + 1.3 \quad (9)$$

The AGN selection criteria are based on the [N II]  $\lambda 6583$  H $\alpha$  ratio and the [O III]  $\lambda 5007$  H $\beta$  ratio. The AGN selection criteria are based on the [N II]  $\lambda 6583$  H $\alpha$  ratio and the [O III]  $\lambda 5007$  H $\beta$  ratio. The AGN selection criteria are based on the [N II]  $\lambda 6583$  H $\alpha$  ratio and the [O III]  $\lambda 5007$  H $\beta$  ratio.

The AGN selection criteria are based on the [N II]  $\lambda 6583$  H $\alpha$  ratio and the [O III]  $\lambda 5007$  H $\beta$  ratio. The AGN selection criteria are based on the [N II]  $\lambda 6583$  H $\alpha$  ratio and the [O III]  $\lambda 5007$  H $\beta$  ratio. The AGN selection criteria are based on the [N II]  $\lambda 6583$  H $\alpha$  ratio and the [O III]  $\lambda 5007$  H $\beta$  ratio.

The AGN selection criteria are based on the [N II]  $\lambda 6583$  H $\alpha$  ratio and the [O III]  $\lambda 5007$  H $\beta$  ratio. The AGN selection criteria are based on the [N II]  $\lambda 6583$  H $\alpha$  ratio and the [O III]  $\lambda 5007$  H $\beta$  ratio. The AGN selection criteria are based on the [N II]  $\lambda 6583$  H $\alpha$  ratio and the [O III]  $\lambda 5007$  H $\beta$  ratio.

## 3 OBSERVATIONS AND ANALYSIS

### 3.1 The group AGN fraction

The group AGN fraction is  $0.01^{+0.29}_{-0.26}$  for groups with  $M_{\text{AGN}} > 9.9 M_{\odot}$ .



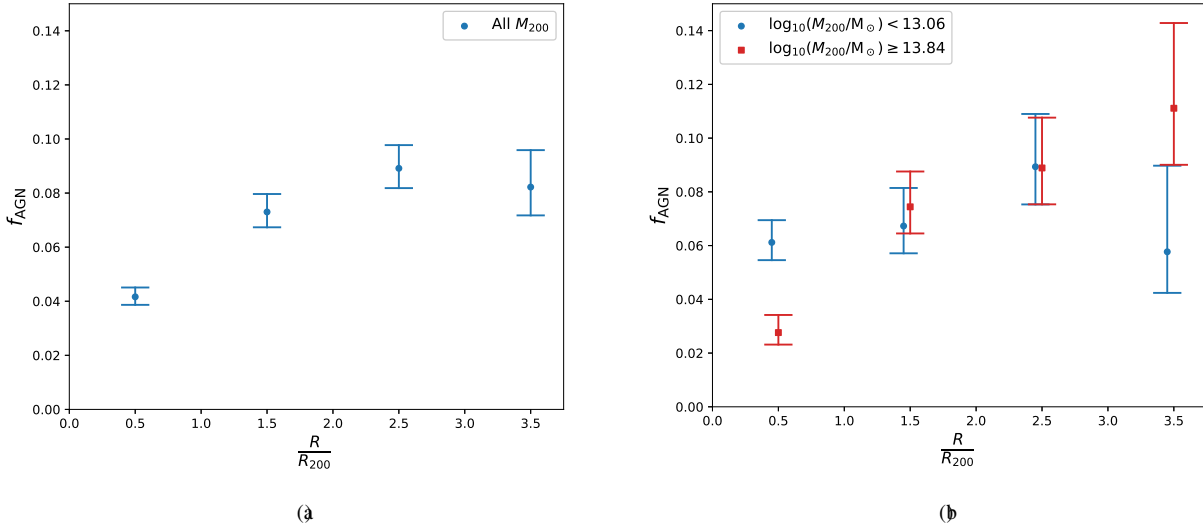


Figure 5. The fraction of AGN in the inner parts of the group. The fraction of AGN in the inner parts of the group is plotted against the normalized radius  $R/R_{200}$ . The data points are shown for all  $M_{200}$  (a) and for two different mass bins:  $\log_{10}(M_{200}/M_{\odot}) < 13.06$  (b) and  $\log_{10}(M_{200}/M_{\odot}) \geq 13.84$  (c).

As a result, the AGN fraction in the inner parts of the group is  $f_{\text{AGN}} \sim 5\%$  (Melia 2006; Atch 2009). This is consistent with the AGN fraction in the inner parts of the group  $f_{\text{AGN}} \sim 7 - 9\%$  (Stra 2007; Atch 2009; Orla 2014; Tikh 2014). Our results show that the AGN fraction in the inner parts of the group is  $f_{\text{AGN}} \sim 6.01^{+0.29}_{-0.26}\%$  for  $0.53 \leq \log_{10}(M_{200}/M_{\odot}) \leq 14.56$ . This is consistent with the AGN fraction in the inner parts of the group  $f_{\text{AGN}} \sim 6.68^{+0.62}_{-0.53}\%$  (Stra 2007; Atch 2009; Orla 2014; Tikh 2014).

#### 4.2 Galaxy location within the group structure

As shown in Figure 5, the AGN fraction in the inner parts of the group is  $f_{\text{AGN}} \sim 5\%$  (Melia 2006; Atch 2009; Orla 2014; Tikh 2014). Our results show that the AGN fraction in the inner parts of the group is  $f_{\text{AGN}} \sim 6.01^{+0.29}_{-0.26}\%$  for  $0.53 \leq \log_{10}(M_{200}/M_{\odot}) \leq 14.56$ . This is consistent with the AGN fraction in the inner parts of the group  $f_{\text{AGN}} \sim 6.68^{+0.62}_{-0.53}\%$  (Stra 2007; Atch 2009; Orla 2014; Tikh 2014).

<sup>2</sup> We use the AGN fraction in the inner parts of the group  $f_{\text{AGN}} \sim 6.68^{+0.62}_{-0.53}\%$  (Stra 2007; Atch 2009; Orla 2014; Tikh 2014).

Figure 6. The fraction of AGN in the inner parts of the group. The fraction of AGN in the inner parts of the group is plotted against the normalized radius  $R/R_{200}$  for two different mass bins:  $\log_{10}(M_{200}/M_{\odot}) < 13.06$  (a) and  $\log_{10}(M_{200}/M_{\odot}) \geq 13.84$  (b).

The AGN fraction in the inner parts of the group is  $f_{\text{AGN}} \sim 5\%$  (Melia 2006; Atch 2009; Orla 2014; Tikh 2014). Our results show that the AGN fraction in the inner parts of the group is  $f_{\text{AGN}} \sim 6.01^{+0.29}_{-0.26}\%$  for  $0.53 \leq \log_{10}(M_{200}/M_{\odot}) \leq 14.56$ . This is consistent with the AGN fraction in the inner parts of the group  $f_{\text{AGN}} \sim 6.68^{+0.62}_{-0.53}\%$  (Stra 2007; Atch 2009; Orla 2014; Tikh 2014). The AGN fraction in the inner parts of the group is  $f_{\text{AGN}} \sim 6.01^{+0.29}_{-0.26}\%$  for  $0.53 \leq \log_{10}(M_{200}/M_{\odot}) \leq 14.56$ . This is consistent with the AGN fraction in the inner parts of the group  $f_{\text{AGN}} \sim 6.68^{+0.62}_{-0.53}\%$  (Stra 2007; Atch 2009; Orla 2014; Tikh 2014).

The AGN fraction in the inner parts of the group is  $f_{\text{AGN}} \sim 5\%$  (Melia 2006; Atch 2009; Orla 2014; Tikh 2014). Our results show that the AGN fraction in the inner parts of the group is  $f_{\text{AGN}} \sim 6.01^{+0.29}_{-0.26}\%$  for  $0.53 \leq \log_{10}(M_{200}/M_{\odot}) \leq 14.56$ . This is consistent with the AGN fraction in the inner parts of the group  $f_{\text{AGN}} \sim 6.68^{+0.62}_{-0.53}\%$  (Stra 2007; Atch 2009; Orla 2014; Tikh 2014).

A similar result

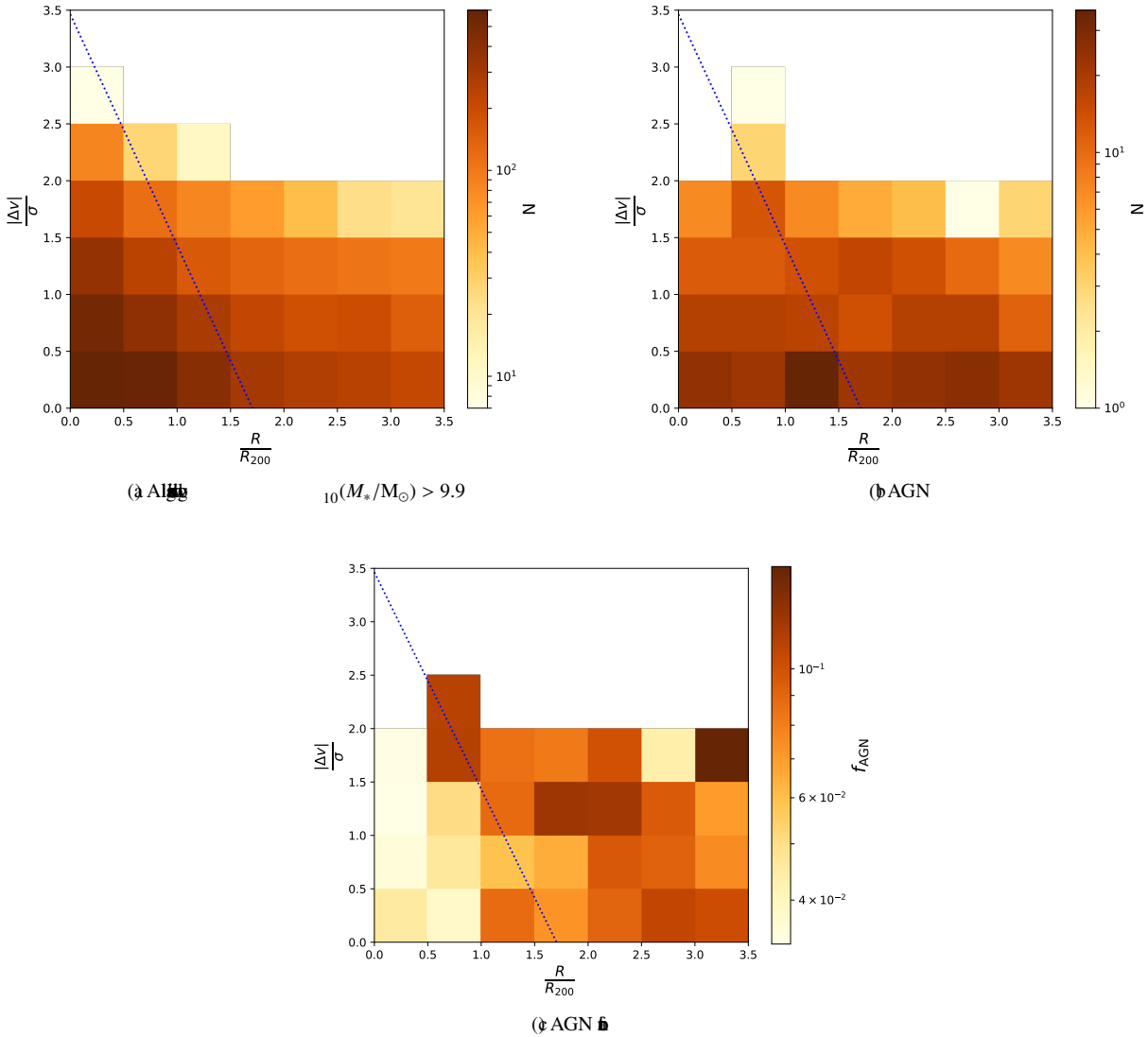


Figure 6. Total number of AGN (a) and non-AGN (b) galaxies, and the fraction of AGN in the field (c) ( $f_{\text{AGN}}$ ) as a function of  $R/R_{200}$  and  $|\Delta V|/\sigma$ . The AGN fraction is  $\sim 0.02$ .

AGN in the field. In the field, the ICM is not present. The AGN fraction is  $\sim 0.02$  (e.g. [Dai & Bin 2016](#); [Dai 2017](#)). As shown in [Shih 2003](#), the AGN fraction is  $\sim 0.02$  in the field.

The AGN fraction in the field is  $\sim 0.02$  (e.g. [Shih 2003](#); [Dai & Bin 2016](#); [Dai 2017](#)). In the field, the AGN fraction is  $\sim 0.02$  (e.g. [Shih 2003](#); [Dai & Bin 2016](#); [Dai 2017](#)).

(e.g. [Katz 2004](#)). Given the AGN fraction in the field is  $\sim 0.02$  (e.g. [Shih 2003](#); [Dai & Bin 2016](#); [Dai 2017](#)), the AGN fraction in the field is  $\sim 0.02$  (e.g. [Shih 2003](#); [Dai & Bin 2016](#); [Dai 2017](#)).

The AGN fraction in the field is  $\sim 0.02$  (e.g. [Shih 2003](#); [Dai & Bin 2016](#); [Dai 2017](#)).

$\sim 7.5$  gal

field



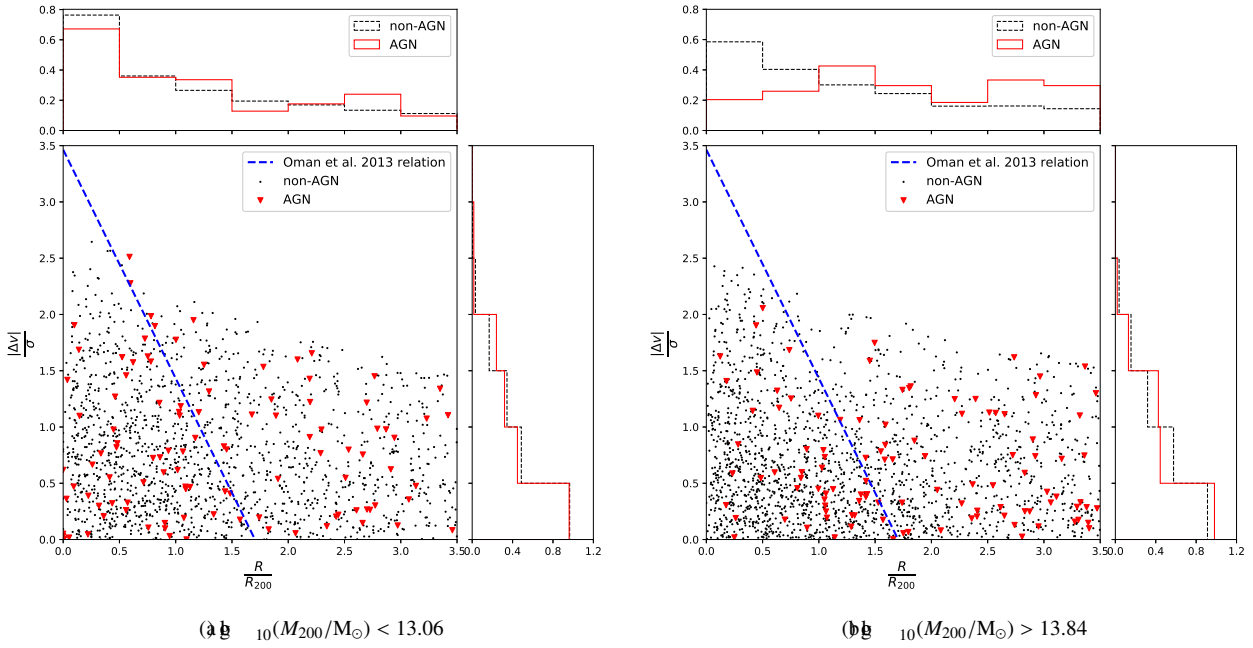


Figure 7. The distribution of AGN and non-AGN galaxies in groups. The top panel shows the fraction of AGN (red solid line) and non-AGN (black dashed line) galaxies. The bottom panel shows the AGN fraction ( $f_{\text{AGN}}$ ) versus the radius  $R/R_{200}$ . The blue dashed line represents the Oman et al. (2013) relation. Black dots represent non-AGN galaxies, and red triangles represent AGN galaxies.

### 4.3 A comparison to radio AGN, star-forming galaxies, and the passive population

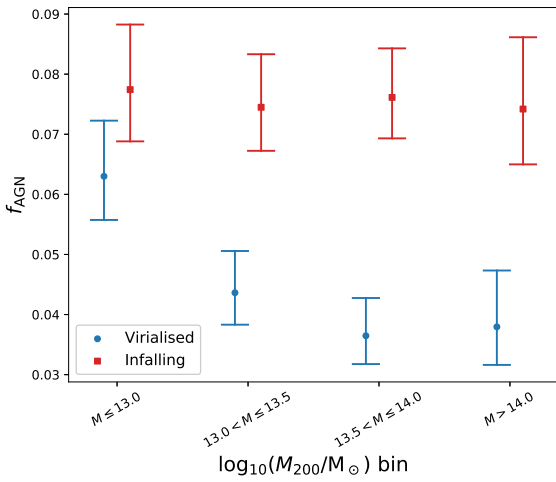


Figure 8. A plot showing the AGN fraction ( $f_{\text{AGN}}$ ) versus the  $\log_{10}(M_{200}/M_{\odot})$  bin. Blue circles represent virialised galaxies, and red squares represent infalling galaxies. Error bars indicate uncertainty.

The AGN fraction is compared to the fraction of radio AGN, star-forming galaxies, and the passive population. The fraction of radio AGN is shown in the top panel, the fraction of star-forming galaxies in the middle panel, and the fraction of the passive population in the bottom panel. The fraction of radio AGN is generally higher than the fraction of star-forming galaxies and the passive population. This is particularly true for infalling galaxies, which show a higher fraction of radio AGN compared to virialised galaxies. The fraction of radio AGN is also higher in groups with higher mass, consistent with the trend seen in Figure 8.

AGN fraction





GR., GM. E., AD., BEP., WEC., MCK.,  
 PJC., BE., 2007, *MNRAS*, 380, 1467  
 GR., HM. P., 1985, *AJ*, 292, 404  
 GR. A., et al., 2017, *MNRAS*, 465, 2671  
 GR. S., et al., 2016, *MNRAS*, 461, 560  
 GM. W., et al., 2017, *AJ*, 153, 111  
 HC. P., et al., 2012, *AJ*, 754, 97  
 HL., et al., 2015, *MNRAS*, 446, 1356  
 HM. J., ED. A., CH. H., 2007, *MNRAS*, 376, 1849  
 HP., 1997, *ARA&A*, 35, 357  
 HA. M., et al., 2013, *MNRAS*, 430, 2047  
 KA. FG., et al., 2003, *MNRAS*, 346, 1055  
 KD. D. P., CH. H., VB., 2004, *AJ*, 127, 3361  
 KL. J., DM. A., SR. S., HC. A., TJ.,  
 2001, *AJ*, 556, 121  
 KY., DH. D., MP., 2002, *AJ*, 572, 169  
 LB., et al., 2015, *MNRAS*, 452, 2087  
 LP. A. A., RA. L. B., RB. B., 2017, *MNRAS*, 472, 409  
 MS., RS., PK. A., 2012, *MNRAS*, 427, 1252  
 MM. A., SH. S., KM. G. H., PK. A., CH.  
 D. J., OM. S., 2018, *MNRAS*, 474, 3615  
 MP., KD. D., KE., MJ. S., AA. A., 2006, *AJ*,  
 644, 116  
 MF. K., 1995, *MNRAS*, 274, 845  
 MB., KN., LG., DA., OA., 1996, *Nu* 379,  
 613  
 ME., BA., BS., MG., FD., 2013, *MNRAS*,  
 430, 2638  
 NF. F., FC. S., WB. D. M., 1996, *AJ*, 462, 563  
 OH., et al., 2014, *AJ*, 790, 43  
 OK. A., HM. J., 2016, *MNRAS*, 463, 3083  
 OK. A., HM. J., BP. S., 2013, *MNRAS*, 431, 2307  
 OL. P., 1980, *C&A* 8, 177  
 OM. S., CW. J., NE. E. J., RS. W., 2012, *AJ*, 750,  
 L23  
 OM. S., et al., 2013, *AJ*, 772, 104  
 OM. S., et al., 2017, *MNRAS*, 468, 1824  
 PL., et al., 2013, *A&A*, 552, A111  
 PK. A., JP. C., 2012, *MNRAS*, 426, 1632  
 PK. A., SH. S., HC. P., FMKA., FD.  
 J. E., 2013, *MNRAS*, 429, 1827  
 PL., RK., BO. O., BC. M., 1996, *AJS*, 104, 1  
 PJ. M., WH., 2000, *AJ*, 529, 157  
 PP. M., et al., 2017, *Nu* 548, 304  
 RC., GM. J., KM. J., DA., 2005, *AJ*, 130, 1482  
 RA. S. G., et al., 2011, *MNRAS*, 416, 2640  
 RA. S. G., et al., 2014, *MNRAS*, 444, 3986  
 RW. C., HD. A., FW. K., 1991, *AJS*, 76, 153  
 RH. T., EH., 2005, *AJ*, 623, L81  
 SH. F., et al., 2017, *RvMe An yA Sth*  
 arXiv:1709.05438  
 SD. B., SB. T., EH. H., MB. F., MK., NG.  
 LG., SN. Z., 1988, *AJ*, 325, 74  
 SH., SC., 2001, *MNRAS*, 328, 185  
 SH., MJ. S., RS., RA., PF. J.,  
 2007, *AJ*, 654, L115  
 SH., KH., SS., SY., 2003, *AJ*, 590, 197  
 SH. J., et al., 2004, *AJ*, 128, 1558  
 SH. G., CF. R., MA., SL., AN. V., 2006,  
*MNRAS*, 371, 972  
 TE. N., et al., 2011, *MNRAS*, 418, 1587  
 TB., BC. L., 2009, *AJ*, 694, 789  
 TP., et al., 2014, *AJS*, 212, 9  
 VM., et al., 2015, *MNRAS*, 452, 3529  
 WT., et al., 2017, *A&A*, 601, A63  
 WD. F., GM. J., 2007, *AJ*, 134, 527

~~http://~~

~~EX/LATEX fit~~